A Hybrid Combining Hard and Soft Robots

A Hybrid Combining Hard and Soft Robots

Adam A. Stokes[1], Robert F. Shepherd[1], Stephen A. Morin[1], Filip Ilievski[1],and George M. Whitesides[1,2]*

[1] Department of Chemistry and Chemical Biology, Harvard University, 12 Oxford Street, Cambridge, MA 02138, USA.

[2] Wyss Institute for Biologically Inspired Engineering, Harvard University, 60 Oxford Street, Cambridge, MA 02138, USA.

(*) Author to whom correspondence should be addressed: gwhitesides@gmwgroup.harvard.edu

Abstract

This manuscript describes a hybrid robotic system combining hard and soft sub-systems. This hybrid comprises a wheeled robot (an iRobot Create©; hard) and a four-legged quadruped (soft). It is capable (using a simple, wireless control system) of rapid locomotion over flat terrain (using the wheeled hard robot), and of gripping and retrieval of an object (using the soft robot). The utility of this system is demonstrated by performing a mission requiring the capabilities of both components: retrieving an object (iPod Nano®) from the center of a room. This class of robot—hybrids comprising hard and soft systems functioning synergistically—is capable of performing tasks that neither can do alone. In contrast to specialised hard robotic arms with grippers (capable of performing some of the functions we describe here), which are complex, relatively expensive, and require sophisticated controls, this hybrid system is easy to construct, simple to control, and low in cost. The soft robotic system in the hybrid is lightweight, disposable if contaminated or damaged, and capable of multiple functions.

1. Introduction

We are developing a class of pneumatic machines—soft robots[1]—that are modelled on invertebrates such as starfish and octopi.[2] At their present (early) level of development, these soft robots usually move slowly, and require pneumatic tethers to a fixed location (e.g., a source of compressed air). They also cannot yet match the load-carrying ability of wheeled or tracked hard robots[3, 4] and are unable to carry the weight of their own electropneumatic control system (EPC).

Compared to complex and relatively expensive hard robots (for example: the tracked "packbot" by iRobot,[5] the hard-robotic quadruped by Hirose et al.,[6] and RHex by Saranli et al.[4]) soft robots have several attractive characteristics: mechanical compliance, low-cost, simple controls enabled by non-linear mechanical properties of materials, light weight and low loading of weight-bearing

surfaces, and low center of gravity.[1, 7] These characteristics may be useful in hazardous, unstable, and toxic environments of the sorts encountered after natural disasters and collapsed buildings. In order to explore, and, potentially, to assist in search and rescue operations within these environments, soft robots must be: i) capable of movement on unstable terrain; ii) capable of directional locomotion; iii) sufficiently inexpensive that they can be abandoned if damaged or contaminated; and iv) capable of carrying sensors, imagers, and samplers (and, ultimately, other capabilities).

We have developed hybrid systems that integrate soft and hard robots, and combine some of the advantages (and circumvent some of the limitations) of each class. The hybrid combines a commercially available wheeled hard robot that can carry loads in excess of 2 kg at 0.5 m/s, and a legged soft robot that is slower (~6.5 m/hr) but capable of movement over unstable terrain, and of versatile gripping. This hybrid can be used in a completely untethered mode: it is controlled wirelessly, and runs on batteries. The hard robot supplies compressed air to the soft robot through a flexible tether, and also carries the controller, microcompressors, and valves that operate the soft robot.

Here we demonstrate the capabilities of the hybrid by using it to retrieve an object from the center of a room, using only a wireless camera and joystick to control the system. We used the rapid movement of the wheeled hard robot to transport the legged soft robot across a room to the object (an iPod nano®) that we wished to retrieve. We deployed the legged robot to walk to and climb over the iPod, and then used the legs of the robot as a gripper to grasp the object. Finally, we drove the hard robot to a new location and, using it, we dragged the iPod in the grip of the tethered soft robot. The tether in this system both provided compressed air to the soft robot, and connected it mechanically to the hard robot.

One feature that distinguishes hard and soft robots is mechanical compliance.[8] Hard robots can be vehicles,[5] arms, grippers, or multi-limbed walking robots.[4, 9] Conventional hard robots share four characteristics: i) they are made of high Young's modulus materials (>100 MPa); ii) they have a fixed number of axes of motion; iii) they do not automatically conform to the surface of objects, or obstacles; and iv) they require sophisticated controls to manipulate objects with complex shapes.

Mechanical compliance is an inherent advantage of soft materials, but their actuation for robotic applications has posed unique challenges. Previously reported soft actuators include: electroactive polymers,[10] shape memory alloys,[11-13] and biosynthetic actuators.[14-16] Actuation of electroactive polymers requires high voltages, shape-memory alloys are relatively slow in rapid cycling, and while biosynthetic actuators have progressed far in the last decade,[14-16] they still require specialized biological processing techniques.

Our soft robots: i) are made of elastomeric materials (<1 MPa Young's modulus) with a variable stiffness that depends on the pneumatic pressurization; ii) can have a non-linear output motion and variable number of axes of motion;[11,12] and iii) require only a simple control system to achieve highly complex motions.

Soft robotics, and soft machines, is a rapidly developing field[8,6,7] that shows promise for applications including gripping and lightweight locomotion. Initial work on soft robotic tentacles by Suzumori et al.[17] has been extended by Martinez et al.[18] to demonstrate mass transport of acid, sand, and salt using a fluidic network. Pneumatically actuated grippers, using highly extensible elastomers, such as those by Ilievski et al.[19] have been shown, with zero feedback in the control loop, to be capable of picking up delicate objects (uncooked chicken eggs and mice). Feedback when gripping using soft machines is possible using compliant, low-cost, sensors such as those by Kramer,[12-14] Mazzeo,[20] and Liu et al.[21] Systems that use a composite of extensible, and inextensible, materials have been shown to be capable of complex motion using simple control inputs.[3,17] Shepherd et al.[22] demonstrated a soft robot that was capable of locomotion by

multiple gaits, and demonstrated a robot undulating below an obstacle. Incorporating fluidic networks into locomoting soft robots allowed Morin et al.[23] to demonstrate both camouflage and display of soft machines. Recent, non-pneumatic, designs of soft robots include the use of shape memory alloy actuators by Lin et al.,[14] and the bioinspired approaches using tissue engineering by Nowroth et al.[15] and Feinberg et al.[16]

1.1 Design of the Hard Robotic Sub-system

Here, we used a wheeled hard robot (iRobot Create©) to carry a power supply, an electro-pneumatic control system, and a quadrupedal soft-robotic walker. The wheeled robot, shown in Figure 2, is capable of traveling at up to 500 mm/s (1800 m/h) on a smooth, flat surface.

1.2 Design of the Electropneumatic Control Sub-system

We created a control system using readily available, low-power microcontrollers, micropumps, and valves so that it would be inexpensive, and able to operate on batteries. We can easily adapt the gait, speed, or direction of the robot by using the microcontroller to alter the state and timing of the pumps and valves. The ability to power this system using batteries is important for portability.

The robot is controlled pneumatically using an array of eight microcompressors and eight valves; each pneu-net is actuated/deactuated using one pump and one valve (Figure 1). We injected compressed air (~7 psi, 0.5 atm, 50 kPa) from each of the eight pump/valve combinations through a silicone tube to each of the pneu-nets. The timing of inflation/deflation of each pneu-net is directed by a program running on a microcontroller. The control system—microcontroller, microcompressors, and valves (Figure 1c)—runs on a 5,200 mAh lithium-polymer battery (7.4V, AT: Tenergy, #18650); the system runs for ~1.5 hours on a full charge, and therefore can be deployed outside the lab.

1.3 Design of the Soft Robotic Sub-system

We created a rotationally (C4) symmetric soft robot that is capable of walking in four directions. The soft robot that we used is a quadruped that is capable of controlled locomotion in four directions at an average speed of 6.5 m/h.

The quadrupedal walker switched between two functions: one locomotive (walking), and one manipulative (gripping). Following the actuation sequence (shown in Figure S6), the robot walked and, by simultaneously actuating all of its legs, functioned like the gripper previously reported.[19]

1.4 Design of the Hybrid System

The hybrid robot, in a marsupial configuration (soft robot carried by hard robot, Figure 2), allowed us to: i) drive the robots, using wheels, quickly over a flat, hard floor to an object (an iPod nano®); ii) walk the legged robot over the iPod; iii) grip the iPod by actuating all four legs at the same time; and iv) pull it to a different location by driving the hard robot.

1.5 Design of the Communications System

We designed the communications system, shown in Figure S1, to allow us to control both robots, wirelessly, using a joystick (eSecure™, USB Dual-Shock Controller) for input. We also included a wireless camera (SecurView™, TrendNet™): this camera, capable of rotation in two axes, allowed us to operate the robot remotely, and did not require us to have direct line-of-sight.

2. Results and Discussion

2.1 Fabrication of the Soft Robot

The quadrupedal soft robot contained two pneu-nets per leg; these actuators allowed us to control the motion of each of the legs, and therefore to drive the robot in four different directions. Acrylonitrile butadiene styrene (ABS) plastic molds were fabricated by fused deposition manufacturing (FDM) in a Dimension Elite 3D printer. Figure S2 provides a technical drawing of the robot. The PN architecture and fabrication methodology is based on the work by Ilievski[19] and Shepherd.[22] We used soft lithography to fabricate the robot using Ecoflex-50 (Smooth-On, Inc.) as the elastomer.

2.2 Building the Hard Robotic Platform and Electro-Pneumatic Control

Figure 2 shows the integrated hybrid system. We controlled this robot using custom software running on a microcontroller (Arduino Mega2560) that outputs serial communications based on iRobot's Open Interface Command (OIC) set.[24] Using the OIC we could: i) control the speed of each of the two wheels; ii) read information back from the built-in sensors on the robot; and iii) use our software to control the electro-pneumatic control (EPC) system. The EPC consists of an array of eight microcompressors and pumps that directed the actuation (inflation/deflation) of the individual pneu-nets in the soft robot. We used the timing of actuation to control the direction of locomotion, or to grip an object.

2.3 Implementation of the Wireless Control System

We used XBee (Sparkfun, WRL-08687) as our wireless communications protocol. We read the input from the joystick using a program running a custom-written script (using the Processing language: processing.org) on a computer. The program sent serial communications over an XBee

link to the wireless communications module (Seeduino Pro & XBee Shield) mounted on the hard robot. We could drive the wheels of the hard robot using the joystick, or we could switch modes and, using the same joystick, control the motion of the soft robot. Figure S1 provides a systems overview of the communications and control sub-systems.

2.4 Multimode Operation of Legged Robot as Gripper

The legged soft robot can also be used to grasp objects (Figure S9). With no sensors on the legs of the robot for feedback, we pressurized all of its actuators to grip a fragile object (a light bulb) without causing damage. This capability is a demonstration of two of the key features of soft robots: multiple functions from a single device, and simple control resulting in complex motion with mechanical compliance.

2.5 Retrieval of an Object

We demonstrated the utility of this hybrid system by using it to retrieve an object: an Apple iPod Nano®. Figure 3 shows still frames from Video S1. Figure 3 a) shows the object in the middle of a room. Using the joystick, we drove the hybrid system across the room at its maximum speed (Figure 3b). In Figures 3c-d) we deployed the soft robot by directing it to walk off the back of the hard robot, and directed it to climb over the iPod. By simultaneously actuating all four legs (all eight pneu-nets) we caused the legged robot to grip the iPod. Finally, (Figure 3e) we showed that, by maintaining the pressure in the soft robot and driving the hard robot away, we could flip the object over, and drag it to a new location. The overturned soft robot acted as a skid and protected the iPod as it was dragged.

3. Conclusions

The hybrid soft-hard robotic system by Dienno et al.[25] used a mobile hard robotic base with a tethered soft robotic trunk. Our system differs in that we have a multifunctional soft robot that is capable of locomotion that is independent of the hard robotic base unit.

This hybrid system is capable of moving rapidly, with no physical connection to the operator, over smooth surfaces using the wheels of the hard robot, and then slowly with the soft robot. The communications system for the hard robot is already well developed. The load-carrying capability of the hard robot enables it to support the components, valves, controllers, and communications systems necessary to run the soft robot. The soft robot is able to walk (albeit slowly), and to grip irregularly shaped objects. The structure of the soft robot, and its connections to the pneumatic tether, enable the combined hard/soft system to provide a protective covering of an object during retrieval, and to move it—once gripped—rapidly. This hybrid of hard and soft robots integrates the benefits of both classes of robots. Systems of this type will allow complex tasks to be performed under remote control, using only relatively simple communication and control systems.

Robots that use this hybrid design may find utility in assisted living (for example by helping elderly or immobile people retrieve objects from the floor that they would otherwise be unable to reach), in search and rescue, for tasks involving some component of a mechanically weak (e.g. wet sand) or underwater path, when access limits the reach of the hard robot (e.g. when it is required to crawl under barriers), and in operation in hazardous environments.
Retrieval of delicate objects by robots has, previously, required precise motion control and feedback. Our system separates this complex control problem into two components: i) the hard robot—which provides rapid motion (over compatible terrain, such as a floor), and carries the weight of the electropneumatic components; ii) the soft robot—which provides a different kind

of motility (for example over sand or mud), and the capability for soft, compliant gripping. Our hybrid system shifts the complexity of the system from the design of control software and sensor feedback systems, into the physical properties of the soft robot: the requirement for precise control and feedback is removed by the introduction of mechanical compliance.

Hybrid hard and soft robotic systems are capable of performing tasks that neither can do alone. While it is true that there are specialised hard robotic arms with grippers that could perform the functions we describe here, those systems are complex, relatively expensive, and require sophisticated controls. Our system, by contrast, is: i) easy to construct; ii) simple to control; and iii) low in cost. The soft robot in our system is lightweight, disposable if contaminated or damaged, and capable of multiple functions.

4. Experimental

4.1 Soft Robot

We purchased Ecoflex-50 from Smooth-on Inc. and used soft lithography to mold the robots as described by Ilievski,[19] Shepherd,[22] and Morin et al.[23]

4.2 Hard Robot and Electro-Pneumatic Control System

We bought a “Create” from iRobot, and controlled it using their proprietary OIC set using software that we ran on an Arduino Mega2560 (DigiKey, #1050-1018-ND). The software code is provided in the Supplemental Materials.

4.3 Wireless Communications

We made a wireless serial communications link using two XBee units (Sparkfun, #WRL-08687). We wrote a custom script (provided in the supplemental materials) using the Processing environment to interpret incoming user commands, from a joystick (eSecure, USB Dual-Shock Controller), and sent this information over the wireless link to the electro-pneumatic control system. We bought a wireless camera (SecurView, TrendNet) and used the manufacturer's web-browser interface to control the orientation remotely and to view the on-robot video stream.

Acknowledgements

This work was supported by the Defense Advanced Research Planning Agency award number W911NF-11-1-0094.

Author Disclosure Statements

No competing financial interests exist.

References

1. Albu-Schaffer, A., et al., Soft Robotics. IEEE Robot. Autom. Mag., 2008. 15(20): p. 20-30.
2. Sherman, I.W., The invertebrates: function and form, a laboratory guide. 2nd ed. 1976, New York: McMillan. 334.
3. Raibert, M., et al., Bigdog, the rough-terrain quadruped robot. Proc. Int. Congr. Int. Fed. Autom. Control, 17th, 2008: p. 10823-21648.
4. Saranli, U., Buehler, M., and E. Koditscheck, D.E., RHex: A Simple and Highly Mobile Hexapod Robot. Int. J. Rob. Res., 2001. 20(7): p. 616-631.
5. Yamauchi, B., PackBot: A Versatile Platform for Military Robotics Proc. SPIE Int. Soc. Opt. Eng., 2004.
6. Hirose, S. and Kato, K., Development of quadruped walking robot with the mission of mine detection and removal-proposal of shape-feedback master-slave arm. IEEE Int. Conf. Robot., 1998. 2: p. 1713.
7. Trivedi, D., et al., Soft Robotics: Biological Inspiration, State of the Art, and Future Research. Appl. Bionics Biomech., 2008. 5(2): p. 99-117.
8. Deepak, T., et al., Soft robotics: Biological inspiration, state of the art, and future research. Appl. Bionics Biomech., 2008. 5.
9. Lee, Y.J. and Bien, Z., A hierarchical strategy for planning crab gaits of a quadruped walking robot. Robotica, 1994. 12(1): p. 23-54.
10. Guggi, K., et al., Energy minimization for self-organized structure formation and actuation. Applied Physics Letters, 2007. 90.
11. Paik, J.K., Hawkes, E., and Wood, R.J., A novel low-profile shape memory alloy torsional actuator. Smart Materials and Structures, 2010. 19(12): p. 125014.
12. Seok, S., et al., Meshworm: A Peristaltic Soft Robot With Antagonistic Nickel Titanium Coil Actuators. IEEE, (99): p. 1-13.
13. Seok, S., et al., A Peristaltic Soft Robot with Antagonistic Nickel Titanium Coil Actuators. IEEE Trans. Mech., 2013. Accepted for publication, to appear.
14. Lin, H.-T., Leisk, G.G., and Trimmer, B., GoQBot: a caterpillar-inspired soft-bodied rolling robot. Bioinspiration Biomimetics, 2011. 6: p. 026007
15. Nawroth, J., et al., A tissue-engineered jellyfish with biomimetic propulsion. Nat. Biotechnol., 2012. 30(8): p. 792-797.
16. Feinberg, A., et al., Muscular thin films for building actuators and powering devices. Science, 2007. 317(5843): p. 1366-1370.
17. Suzumori, K., Iikura, S., and Tanaka, H. Development of Flexible Microactuator and its Applications to Robotic Mechanisms. in IEEE Int. Conf. Robot. 1991. Sacramento, California.
18. Martinez, R.V., et al., Robotic Tentacles with Three-Dimensional Mobility Based on Flexible Elastomers. Adv. Mater., 2012: p. 1-8.
19. Ilievski, F., et al., Soft Robotics for Chemists. Angew. Chem. Int. Ed., 2011. 50: p. 1890-1895.
20. Mazzeo, A.D., et al., Paper-Based, Capacitive Touch Pads. Adv. Mater., 2012. 24(21): p. 2850-2856.
21. Liu, X., et al., Paper-based piezoresistive MEMS sensors. Lab Chip, 2011. 11: p. 2189.

22. Shepherd, R., et al., Multigait soft robot. Proc. Natl. Acad. Sci. U. S. A., 2011. 108(51): p. 20400-20403.
23. Morin, S., et al., Camouflage and display for soft machines. Science, 2012. 337(6096): p. 828-832.
24. iRobot, iRobot Create Open Inter face (OI) Specification. 2006, www.irobot.com.
25. Dienno, D., Design and analysis of a soft robotic manipulator with base rotation. Masters Thesis, U. Penn., 2006.
26. Kramer, R.K., et al., Soft curvature sensors for joint angle proprioception. ICROS, 2011: p. 1919-1926.
27. Kramer, R.K., Majidi, C., and Wood, R.J., Wearable tactile keypad with stretchable artificial skin. IEEE Int. Conf. Robot., 2011: p. 1103-1107.
28. Majidi, C., Kramer, R., and Wood, R., A non-differential elastomer curvature sensor for softer-than-skin electronics. Smart Mater. Struct., 2011. 20(10): p. 105017.
29. Martinez, R., et al., Robotic Tentacles with Three-Dimensional Mobility Based on Flexible Elastomers. Adv. Mater., 2012.
30. Buchli, J. and Ijspeert, A.J., Self-organized adaptive legged locomotion in a compliant quadruped robot. Auton. Robot., 2008. 25(4): p. 331-347.
31. Williams, T.L., Experimental analysis of the gait and frequency of locomotion in the tortoise, with a simple mathematical description. . J. Physiol., 1981. 310: p. 307-320.
32. Rogers, J.A. and Nuzzo, R.G., Recent progress in soft lithography. Mater. Today, 2005. 8(2): p. 50-56.
33. Xia, Y. and Whitesides, G.M., Soft lithography. Annu. Rev. Mater. Sci., 1998. 28(1): p. 153-337.

Figure 1. a) A plan-view schematic of the design of the pneu-net based quadrupedal soft robot. Each of the four legs contains two independently actuated pneu-nets. A full technical drawing is provided by Figure S2. b) A system diagram showing the pneumatic and electrical control system. c) A photograph showing the soft robot, pneumatic tether, microcontroller and pneumatic control system.

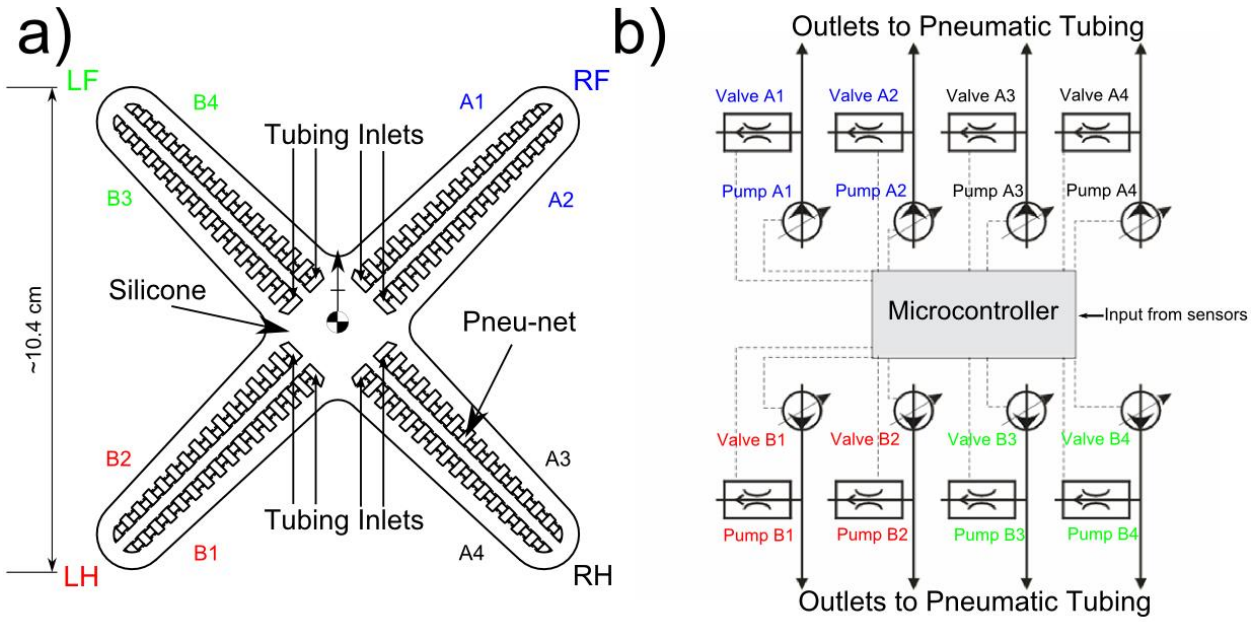
a)
LF
RF
B4
A1
Tubing Inlets
B3
A2
Silicone
Pneu-net
~10.4 cm
B2
A3
Tubing Inlets
B1
A4
LH
RH
b)
Outlets to Pneumatic Tubing
Valve A1
Valve A2
Valve A3
Valve A4
Pump A1
Pump A2
Pump A3
Pump A4
Microcontroller
Input from sensors
Valve B1
Valve B2
Valve B3
Valve B4
Pump B1
Pump B2
Pump B3
Pump B4
Outlets to Pneumatic Tubing

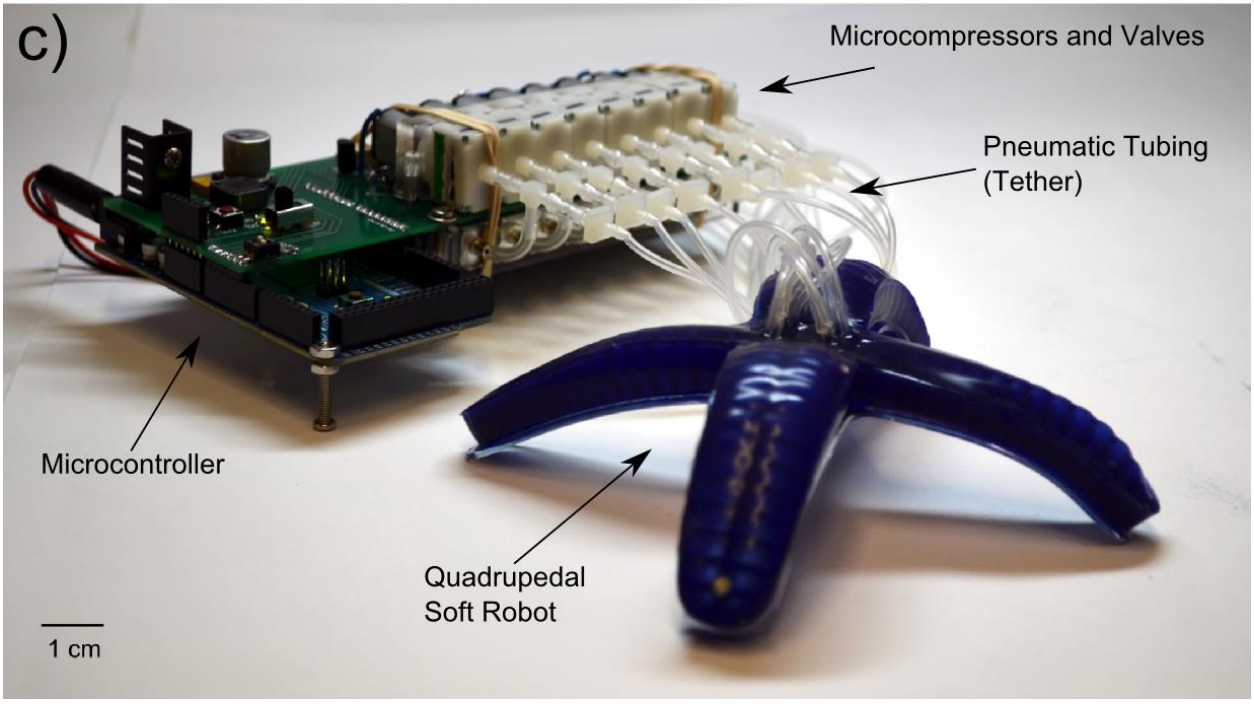
c)
Microcompressors and Valves
Pneumatic Tubing
(Tether)
Microcontroller
Quadrupedal
Soft Robot
1 cm

Figure 2. A photograph of the hybrid robotic platform showing the wheeled hard robot (iRobot Create©) and the legged soft robot. The hard robot carried, in marsupial fashion, the legged soft robot, the electro-pneumatic control system, and the wireless communications system. This figure does not show the wireless camera that was mounted on the hard robot.

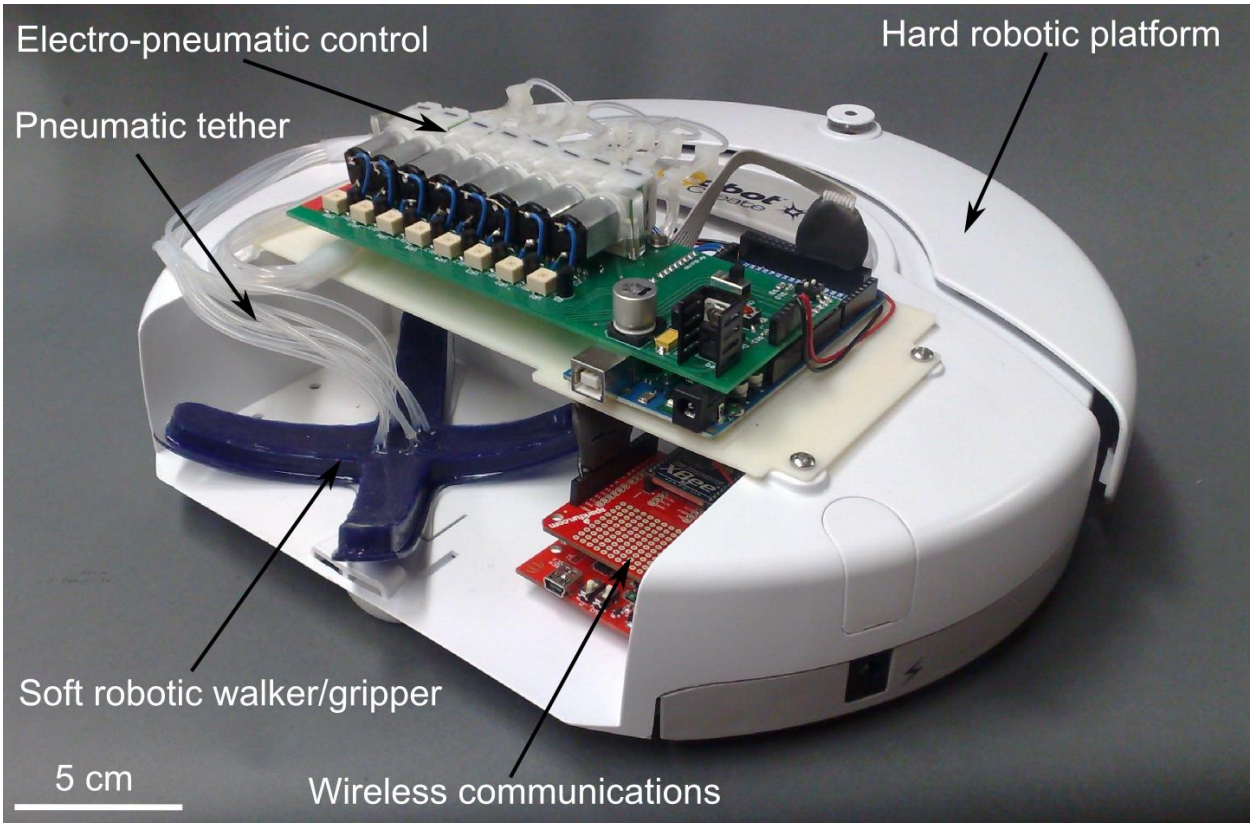
Electro-pneumatic control
Hard robotic platform
Pneumatic tether
Soft robotic walker/gripper
5 cm
Wireless communications

Figure 3. A series of still-frames, from Video S1, show the hybrid robotic system retrieving an object (iPod Nano®) from the centre of a room (a-f). The hard robot carries the soft robot to the object (b). The soft robot, first acts as a walker (c-d), and then as a gripper (e). When the hard robot is driven away (f), the soft robot inverts, and protects the iPod as it is pulled to a new location.

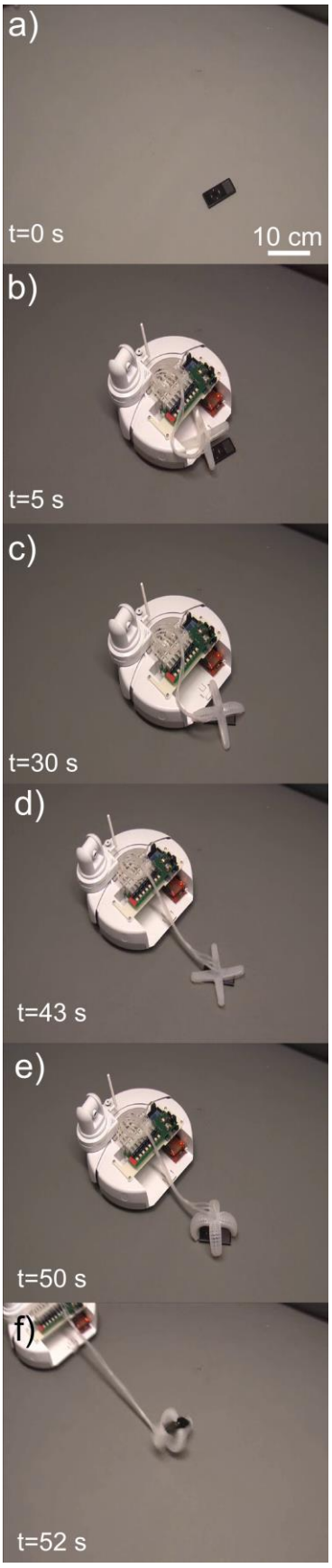
a)
t=0 s
10 cm
b)
t=5 s
c)
t=30 s
d)
t=43 s
e)
t=50 s
f)
t=52 s

A Hybrid Combining Hard and Soft Robots

Adam A. Stokes, Robert F. Shepherd, Stephen A. Morin, Filip Ilievski, and George M. Whitesides*

SUPPLEMENTAL INFORMATION

Department of Chemistry and Chemical Biology, Harvard University

12 Oxford Street, Cambridge, MA 02138

*Corresponding author, email: gwhitesides@gmwgroup.harvard.edu

Multimedia

Video S1: Retrieval of an object by the hybrid system

Video S2: Gripping of a lightbulb by the soft robot

Video S3: Directional control of the robot

Video S4: Motion capture analysis of the soft robot walking on a flat surface

Video S5: The soft robot walking on sand

Video S6: Motion capture analysis of the soft robot walking on sand

Video S7: The soft robot climbing an inclined surface

Technical Files

SI PCB CAD Files.zip contains:

The PCB gerber files.

The laser cutting CAD files for the microcompressor/valve mounting racks.

The bill of materials for the electronics components required to populate the PCB.

The source code.

Supplemental Design Details

S1.1 Design of the soft robotic sub-system

Our legged design allows us to drive the robot over sand, and up inclines. For actuation, we incorporated a double pneu-net structure into each of the four legs. This network allowed movement in any direction across a surface. These robots used a battery-powered electro-pneumatic control system that included valves and pumps taken from low-cost (~$10), commercial blood-pressure monitors used for home health-care. We have also implemented paper-based piezo-MEMS bump sensors [8], so that the control system of the robot can alter its course autonomously based on feedback from its environment. An alternative type of soft sensor has been developed by Kramer and Majidi et al.[26-28]; it uses liquid metal alloy networks, embedded in elastomers; this sensing mechanism could be used in future designs of soft robots.

The soft robot we describe here is inexpensive, versatile, and autonomous. Although still tethered, this design has two important advantages useful in exploring unstable terrain; the tethers allow: i) heavy and more expensive components to remain off-board and ii) the possibility of transferring liquids/gases/foams/granules from a remote location along the tether, and to or from the soft robot. The capability of mass transport has been used by Morin et al. [4] to camouflage or display a soft robot, and by Martinez et al. [29] to move acid, sand, and salt using a tentacle-like fluidic system.

S1.2. Design of the quadruped

We designed a quadrupedal soft robot that can be steered in four directions. It is 15 cm in length, measured diagonally across its center (Figure S2). The robot contains two parallel pneu-nets in each of the four legs; these pneu-nets run from the center of the body to the tip of the leg. The parallel pneu-nets allow us to actuate each leg in a "paddling" motion using three steps (Figure S3a-d): i) both pneu-nets are, initially, at atmospheric pressure; ii) the tip of the leg moves forward-and-down by inflating pneu-net 1; iii) the same tip then moves down-and-back by inflating both pneu-nets; iv) it then moves upward-and-backwards by deflating pneu-net 2; v) the leg returns to its initial position by deflating both pneu-nets. The actuation/deactuation sequence of each of the four legs determines the direction of the robot.

The robot is C4 rotationally symmetric. Interestingly, nature rarely adopts this body plan: it is found only in certain jellyfish and some plants.[2] We chose this design because it allows the robot to move across a surface in four directions of travel, and the symmetry simplifies the design of the control system. The symmetric design eliminates the need for the robot to turn-in-place (as for other quadrupedal[30] and wheeled or tracked robots[5])—the control system simply redefines which side of the robot is now acting as the "front."

S1.3. Design of the pneumatic control system

We designed the printed circuit board (PCB) for the controller in-house, and it was fabricated by a commercial vendor (my4pcb.com.) The PCB provides the circuitry to run the microcompressors and valves (both sourced from commercial sphygmomanometers: $12 for one valve and one pump.) We programmed a microcontroller (Arduino Mega2560, DigiKey # 1050-1018-ND) to provide the control signals

S1.4. Design of the actuation sequence

Since the robot is rotationally symmetric, it has no front, back, or side. The gait of the robot is controlled by the direction of paddle of each leg, and the timing offset between the actuation of each leg. The gait we employ is similar to that used by tortoises and other slow-moving quadrupedal animals[31]; Figure S6.

S1.5. Design of the paper-based bump sensors for feedback

For these robots to operate in terrain more complex than an open, flat surface, they must be able to sense their surroundings. For closed-loop feedback in the robotic system, we chose paper-based piezoresistive MEMS sensors[20, 21] because they are inexpensive and easy to fabricate. The sensors allowed the control system to adapt the direction of locomotion of the robot to the presence of obstacles. For example, if the sensor touched an obstacle such as a wall, the control system could respond by reversing the direction of locomotion to avoid contact with the object before trying a new direction. We designed a sensor network that comprises a four-armed paper origami structure. Each sensor arm has, at its tip, a flexible hinge that is patterned with carbon ink via stenciling to form a bump sensor. Bending one of the flexible paper structures leads to a change in resistance of the piezoresistive carbon sensor. We threshold the output from each sensor, as it is read by the analog to digital (ADC) converter in the microcontroller, to give a binary (on/off) input to the control software.

Using a die-cutting machine (Silhouette Cameo) we created a system of paper origami-carbon ink bump sensors on Whatman 3MM chromatography paper, 340 μm thick, 186 gm-2.
We designed the net to fold up along perforated lines into triangular tube sections, for rigidity (Figure S10b). We made a stencil by laser cutting a thin acetate sheet and used carbon black ink to print four piezoresistive sensors at the hinged section of each arm (Figure S10a). Using silver epoxy, we affixed thin enameled copper wires to the sensors, and routed the wire bundle alongside the pneumatic tether to the control board (Figure S10c).

Supplemental Fabrication Details

S2.1. Fabrication of the soft robot

We fabricated the robots using soft lithography[32, 33] following protocols we have reported previously[19, 22]. We designed the tip of each leg to be rounded to allow a smooth rolling motion of the tip with the surface on which the robot is moving (Figure S2). This architecture was critical for walking on sand. We demonstrated that the quadrupedal soft robot can walk in any of four directions.
We printed ABS molds by fused deposition modeling (FDM) in a Dimension Elite 3D printer (Stratasys, Inc., Eden Prairie, MN). We mixed poly(dimethylsiloxane) (PDMS) pre-polymer (Sylgard 184, Dow) 10:1 w:w with curing agent in accordance with the manufacturer's instructions. We cast 4 mm thick sheets of PDMS on glass and cured them at 80 °C for 4 hours. We mixed the two parts of Ecoflex (Ecoflex 00-50, Smooth-On Inc.) 1:1 v:v at room temperature. We dissolved approximately 10 mg of crystal violet dye (tris(4-(dimethylamino)phenyl)methylium chloride, VWR # 101109-608) in 25 mL of dichloromethane and mixed this solution into the ecoflex silicone pre-polymer. We degassed the ecoflex/dye mixture for 5 min, poured it into the ABS mold, and then cured it at 80 °C for 20 min in a convection oven. We demolded the robot and bonded it, using PDMS pre-polymer, to the 4 mm thick PDMS sheets, we cured the robot for 24 h at room temperature. We then cut the robot from the glass and, using a cannula, we inserted silicone tubing into each pneu-net.

S2.2. Fabrication and programming of the electromechanical control system

We used a home-built control system—a printed circuit board, simple circuitry, a microcontroller, and a series of microcompressors and valves—to operate the robots. We programmed the microcontroller to execute a series of maneuvers. Figure S4 (still-frames from Video S3) shows a robot walking clockwise, in a rectilinear pattern. The robot changes direction, as described earlier, with no physical turning of the robot.

Printed circuit boards were designed in-house and manufactured by my4pcb.com. The PCB CAD files, and bill of materials for the electrical components, are provided as files. The PCB was designed to fit the popular Arduino microcontroller platform.

S2.3. Walking on sand and up an incline

We designed this robot to be light weight and to have a low center-of-gravity; these attributes enable it to traverse unstable terrain. Figure S7b shows a still frame from Video S5 of a robot walking on sand. These robots can also navigate a shallow incline. Figure S7a (a still frame from Video S7) shows a robot climbing a ramp covered with a sheet of paper. The robot is shown at its maximum climbing angle (~15°); on steeper inclines it loses traction. These demonstrations suggest possible designs for specific types of terrain.

S2.4. Acquisition of motion tracking data

To track the position of the robot, we read individual frames from Video S3 and Video S5 into Matlab ®. Firstly, we selected the blue channel from the RGB image and inverted the image intensities; the blues then became bright and the rest of the image dark. Secondly, we thresholded the image so that the only information in the image was that of the robot. Finally, we found the center of pixel intensity (i.e., the robot's center of mass) using the 'centroid' subroutine of regionprops (prepackaged code within Matlab ®) and tracked this centroid in all image frames.

We performed motion tracking analysis on the video of the directionally controlled robot (Video S4) and also on the video of the robot walking on sand (Video S6). Using the motion-tracking data, we determined that the quadrupedal soft robot is capable of walking in any of the four directions at an average speed of 6.51 m/h (~62 body lengths/hour; Video S3). Figure S5 provides the processed distance-time plots: S5a shows the X-axis location of the robot as a function of time, the origin is defined as the upper left-most corner of the frame; S5b shows the corresponding Y-axis data. We plotted linear regression lines to these data and extracted the average speed in each of the four corresponding directions shown in Figure S5: 7.2, 6.3, 5.9, and 6.7 m/h. We performed a similar analysis for the robot walking on sand (Figure S8); on this surface, the robot moves at 5.0 m/h (~50 body lengths/hour), approximately 80% of the velocity on a hard flat surface.

S2.5. Fabrication of the piezoresistive paper sensors

Using a die-cutting machine (Silhouette Cameo) we created paper origami-carbon ink bump sensors (Figure S10). The control system measures the resistance of the carbon ink in the sensors—this resistance changes as a function of the angle of flex at the hinge[21]—and uses the measurement to determine if the robot needs to change course. The bump-sensors show proof of concept in allowing the robot to move reactively—it can alter its course due to interaction with an object, such as a wall. Figure S10c shows the bump-sensor network mounted on the robot, the pneumatic tether, and the electrical tether. The total cost of the control system is approximately $150; the robot, plus sensor network, costs approximately $5.

Figure S1. A block-diagram of the distributed control system. The main program runs on an Arduino MEGA 2560 microcontroller on the electro-pneumatic control (EPC) board. The EPC uses serial communications to direct the motion of the iRobot Create©. An XBee wireless communications system runs on another Arduino microcontroller where it passes commands to and from the EPC and a remote computer. The soft robot connects to the EPC via a pneumatic tether and it is controlled using an array of microcompressors and valves carried by the hard robot. A wireless camera, capable of two axes of rotation, is mounted on the hard robot; it communicates with the remote computer via a WiFi link.

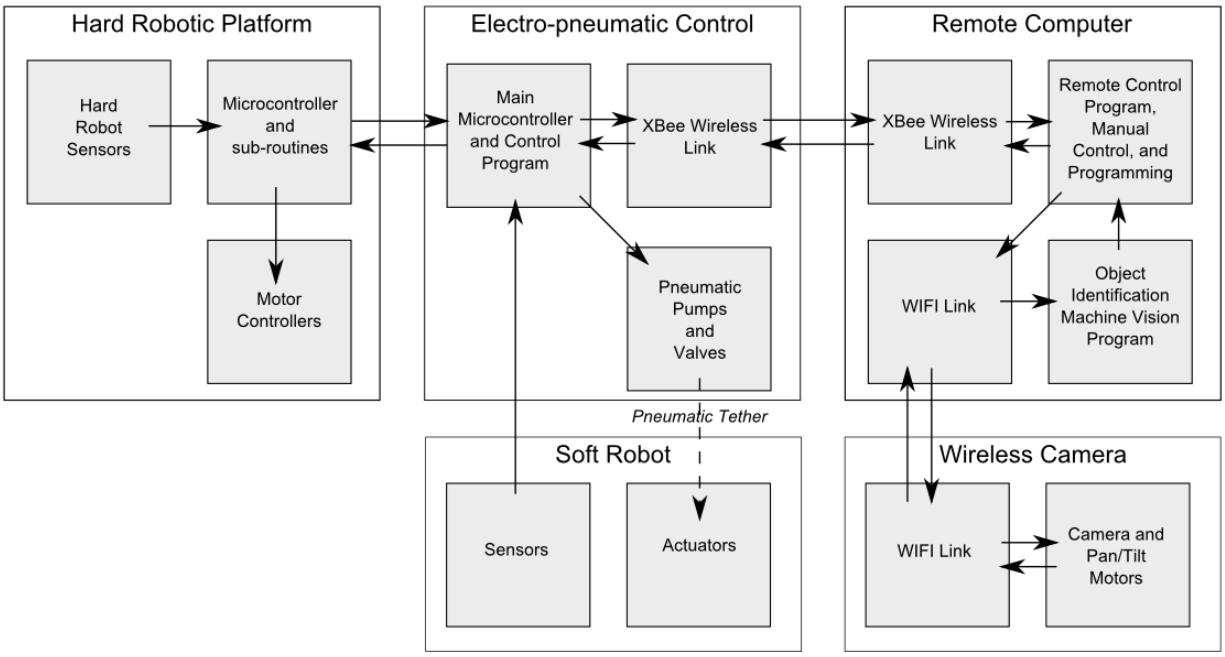
Hard Robotic Platform
Hard Robot Sensors
Microcontroller and sub-routines
Motor Controllers
Electro-pneumatic Control
Main Microcontroller and Control Program
XBee Wireless Link
Pneumatic Pumps and Valves
Pneumatic Tether
Soft Robot
Sensors
Actuators
Remote Computer
XBee Wireless Link
Remote Control Program, Manual Control, and Programming
WIFI Link
Object Identification Machine Vision Program
Wireless Camera
WIFI Link
Camera and Pan/Tilt Motors

Figure S2. A technical schematic of the ecoflex body plan of the quadrupedal robot. Dimensions are in millimeters.

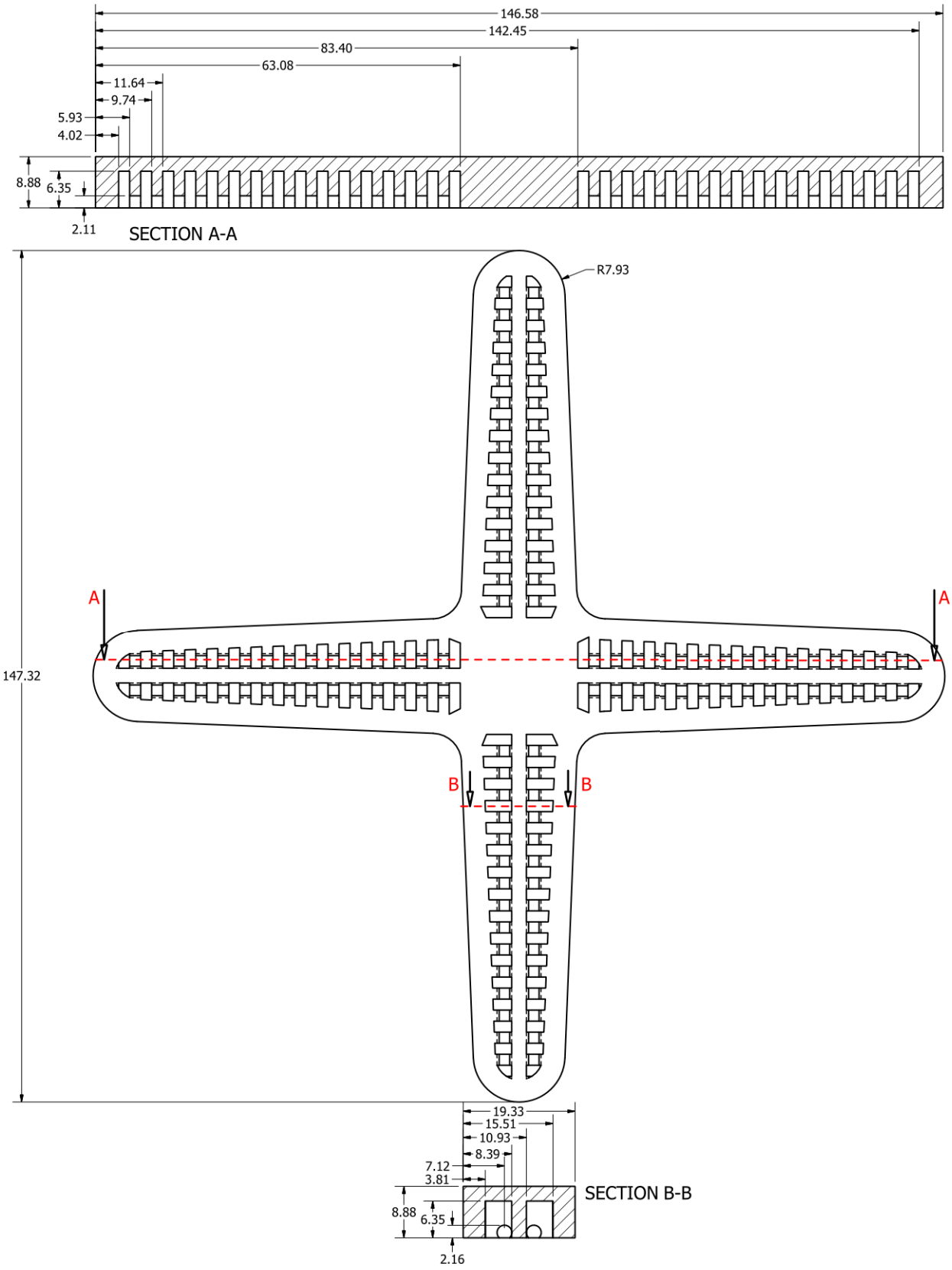
146.58
142.45
83.40
63.08
11.64
9.74
5.93
4.02
8.88
6.35
2.11
SECTION A-A
R7.93
A
A
147.32
B
B
19.33
15.51
10.93
8.39
7.12
3.81
8.88
6.35
2.16
SECTION B-B

Figure S3. A sequence of photographs demonstrating the paddling motion of one of the robot's legs. Pneu-nets are labeled PN for clarity. a) pneu-net 1 and pneu-net 2 are initially at atmospheric pressure. b) pneu-net 1 is inflated to 5 psi, the tip of the leg moves forward-and-down. c) pneu-net 1 and pneu-net 2 are inflated, the leg moves down-and-back. d) pneu-net 1 is deflated, the leg moves back-and-up. The sequence then repeats, pneu-net 1 and pneu-net 2 are deflated, and the leg returns to the position shown in a).

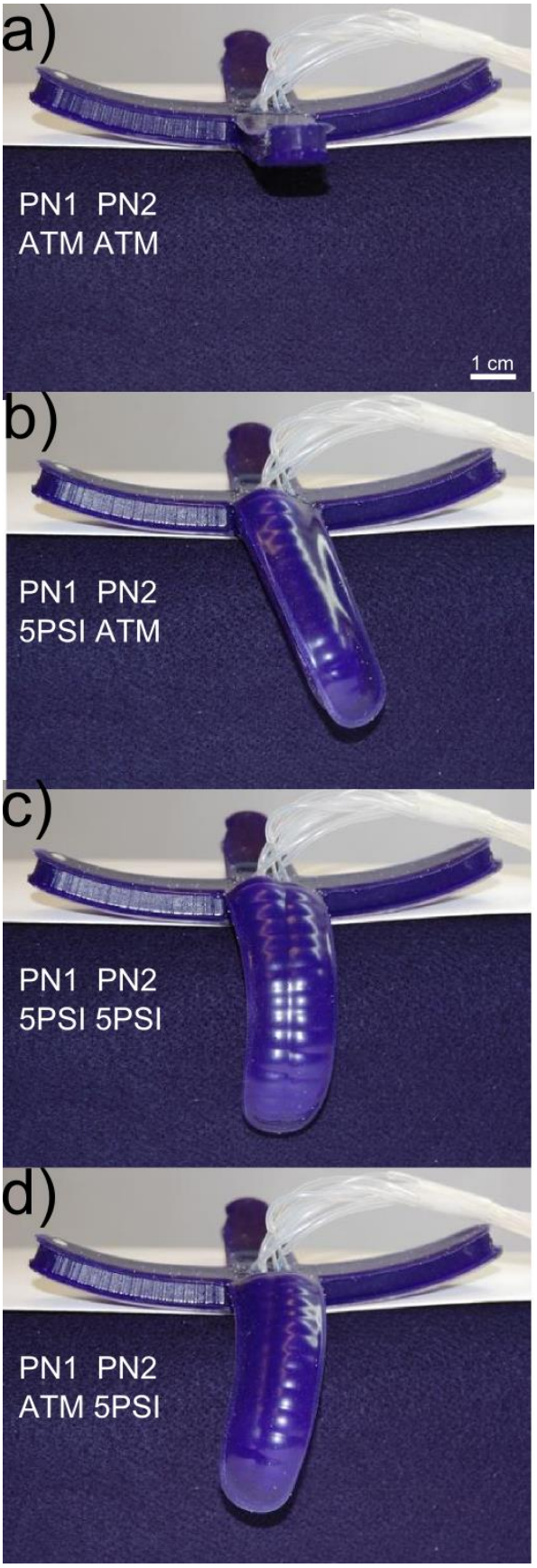
a)
PN1 PN2
ATM ATM
1 cm
b)
PN1 PN2
5PSI ATM
c)
PN1 PN2
5PSI 5PSI
d)
PN1 PN2
ATM 5PSI

Figure S4. Programming the microcontroller to direct the robot along a clockwise square path. This figure shows a composite image of four still-frames from Video S1. The robot starts in the lower left corner of the figure at t=0 s; snapshots show the robot as it walks to the upper left, upper right, and then lower right of the frame; at t=50 s, 102 s, and 158 s respectively. The colored stars correspond to the initial orientation of the robot: left hind, left fore, right fore and right hind are colored in red, green, blue, and black respectively. These stars were applied to the image (they were not physically on the robot) and were added to help in orienting the robot. The effective front of the robot is controlled by the pneu-nets actuated by the microcontroller; the quadruped does not physically turn.

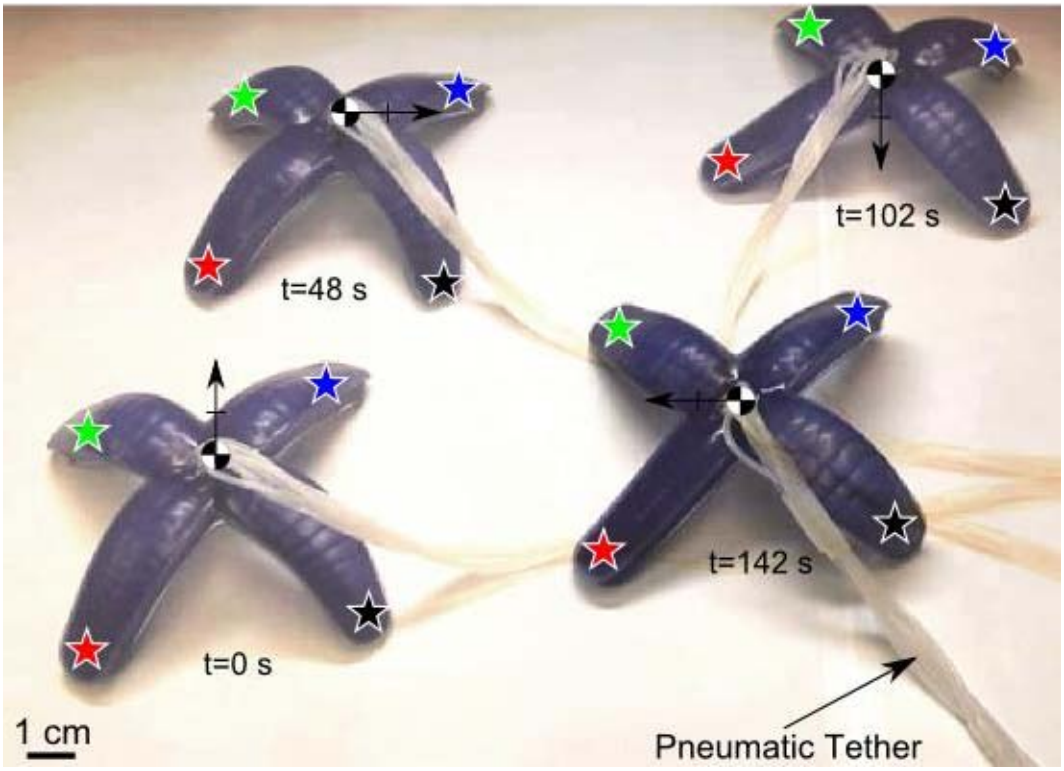
t=48 s
t=102 s
t=0 s
t=142 s
1 cm
Pneumatic Tether

Figure S5. Motion tracking data from Video S3. a) Y position of the centre of mass of the robot with respect to the origin (upper left of the video frame). The calculated Y direction velocities are -0.2, -0.03, 0.16, and -0.01 cm/s. b) X position of the centre of mass of the robot. The calculated X direction velocities are 0.03, 0.17, -0.05, and -0.18 cm/s. The combined X and Y velocities correspond to total speeds of 7.15, 6.34, 5.90, and 6.65 m/h. The average speed of the robot in any direction is, therefore, 6.51 m/h or 62 body lengths per hour.

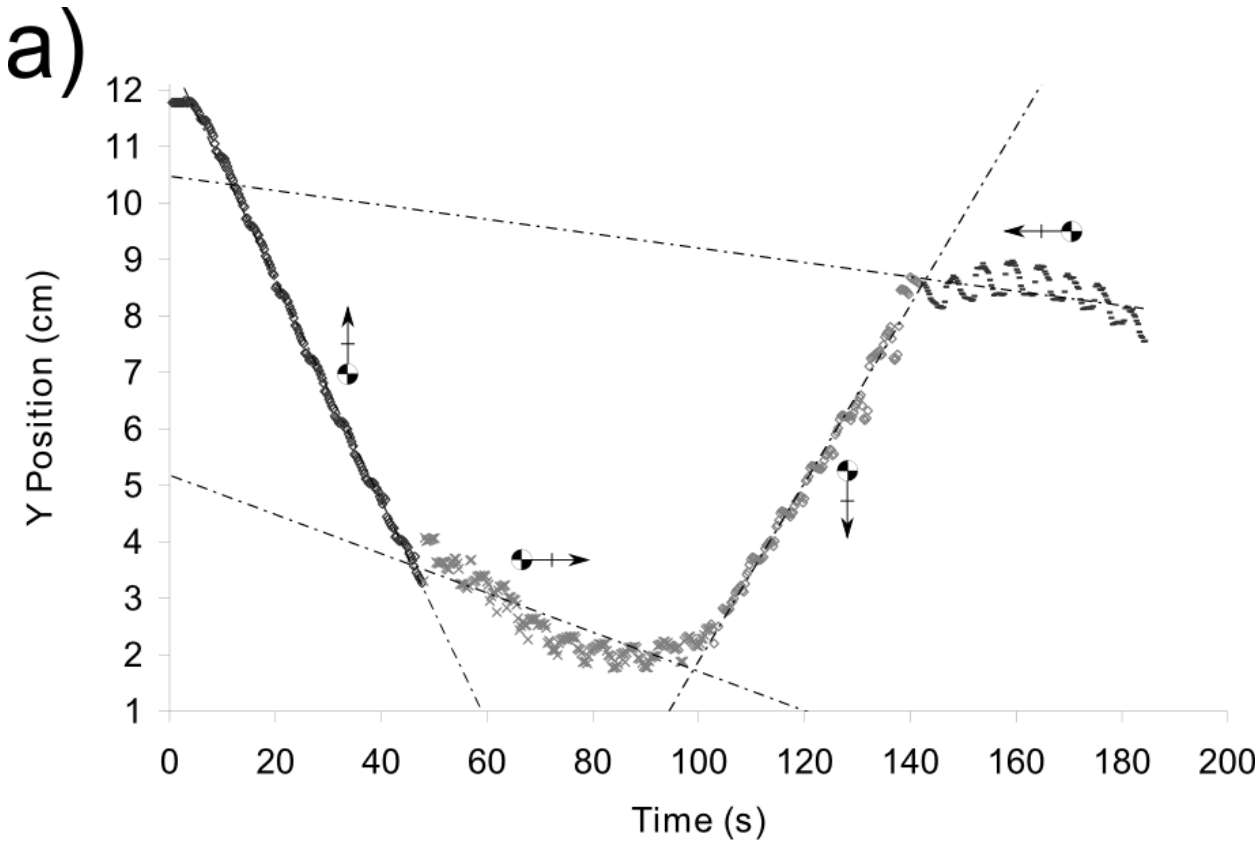
a)
Y Position (cm)
12
11
10
9
8
7
6
5
4
3
2
1
0
20
40
60
80
100
120
140
160
180
200
Time (s)

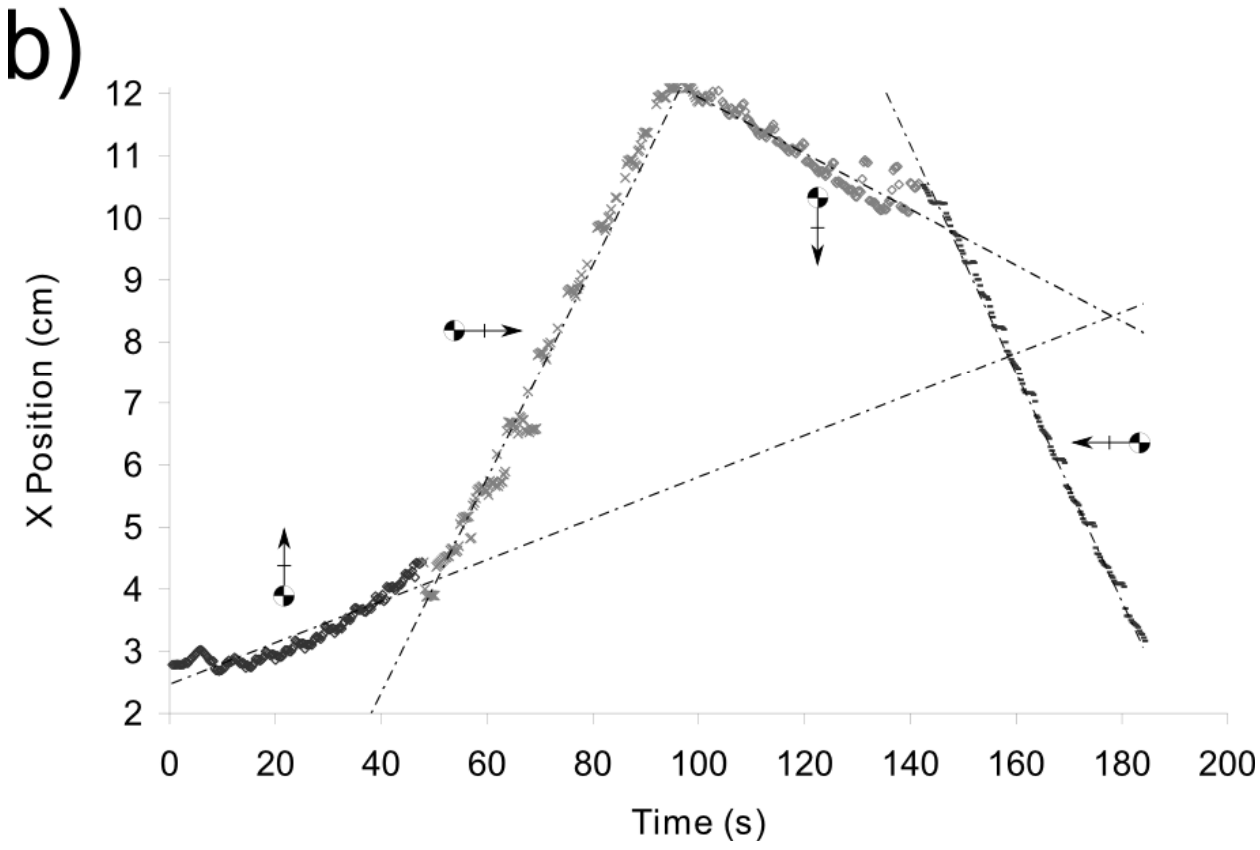
b)
X Position (cm)
12
11
10
9
8
7
6
5
4
3
2
0
20
40
60
80
100
120
140
160
180
200
Time (s)

Figure S6. a) This diagram shows the timing of switching, on and off, of the pumps and valves that results in motion of the robot along the RF-LF axis. b) By rotating the timing diagram it is possible to redefine which side of the robot becomes the effective front of the robot. We have split the timing diagram into nine time sections and so we use mode-9 matrix rotations. For example, a rotation of two means that the timing diagram is shifted two units to the left. The leftmost two elements would “rotate” and re-join the matrix on the right-hand side. Shown here are the leftward-matrix rotations that result in four directions of locomotion without changing the physical orientation of the soft robot.

a)

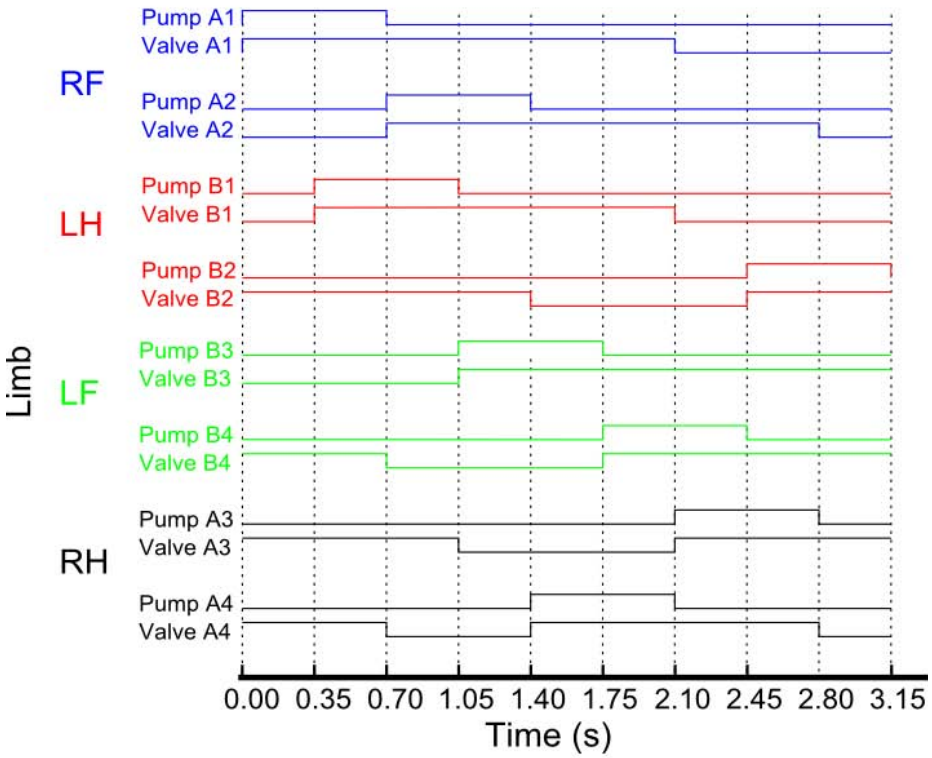

b)

Timing Diagram Rotations

Walking Direction

Limb					
	Pump A1 Valve A1	**9-0 = 9**	9-3 = 6	9-1 = 8	9-6 = 3
LF	Pump A2 Valve A2	9-2 = 7	9-5 = 4	9-7 = 2	9-7 = 5
	Pump B1 Valve B1	9-1 = 8	9-6 = 3	**9-0 = 9**	9-3 = 6
RH	Pump B2 Valve B2	9-7 = 2	9-4 = 5	9-2 = 7	9-5 = 4
	Pump B3 Valve B3	9-3 = 6	9-1 = 8	9-6 = 3	**9-0 = 9**
RF	Pump B4 Valve B4	9-5 = 4	9-7 = 2	9-4 = 5	9-2 = 7
	Pump A3 Valve A3	9-6 = 3	**9-0 = 9**	9-3 = 6	9-1 = 8
LH	Pump A4 Valve A4	9-4 = 5	9-2 = 7	9-5 = 4	9-7 = 2

Figure S7. a) A still-frame from Video S5, showing the robot at the maximum angle of incline (~15°) that it can navigate before losing traction. The surface is paper. b) A still-frame from Video S2 showing the robot navigating an unstable granular terrain: sand.

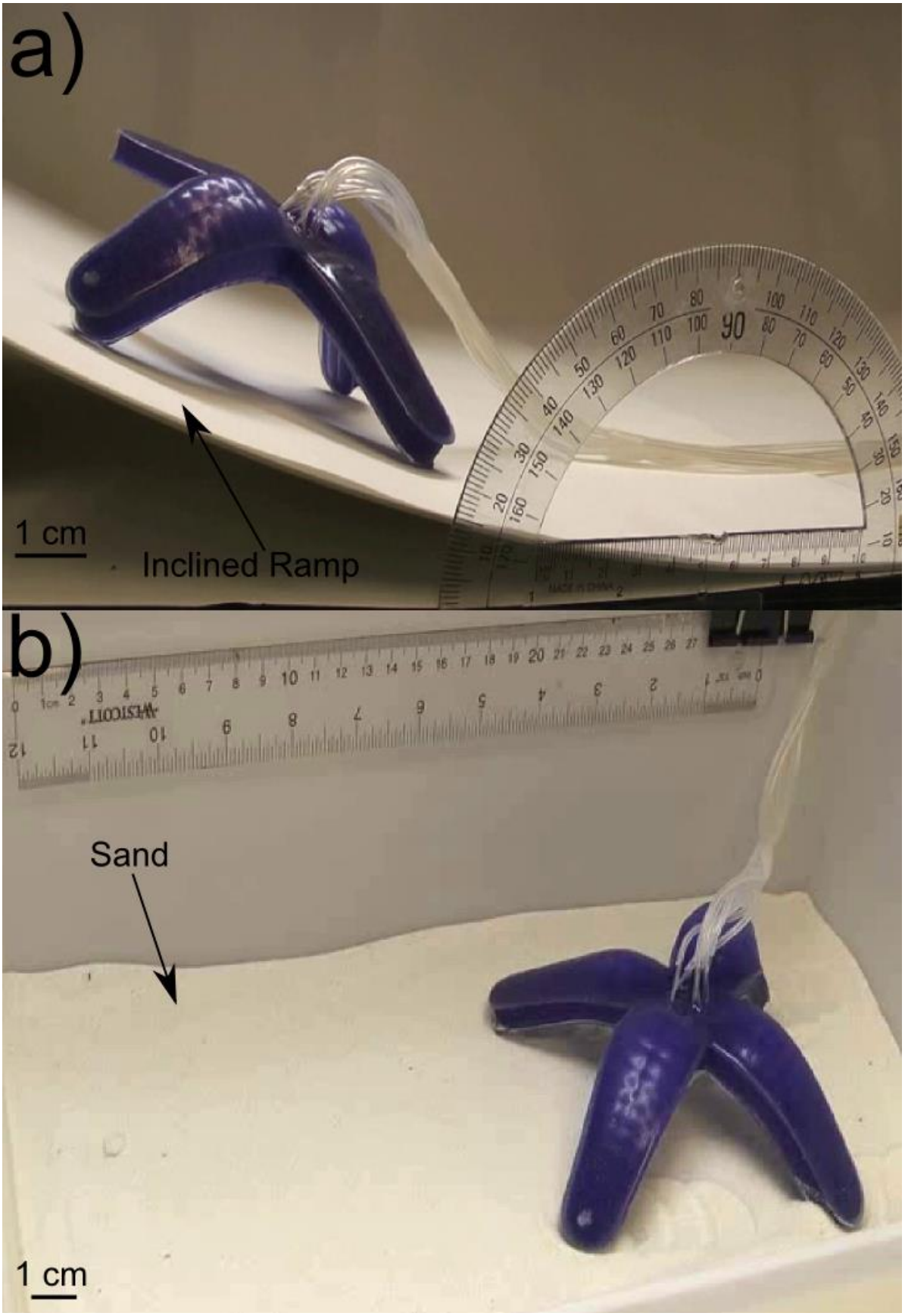
a)
1 cm
Inclined Ramp
b)
Sand
1 cm

Figure S8. Motion tracking data from Video S5. a) Y position of the centre of mass of the robot with respect to the origin (upper left of the video frame). The calculated Y direction velocity is -0.14 cm/s. b) X position of the centre of mass of the robot. The calculated X direction velocity is 0.01 cm/s. The combined X and Y velocities, for the robot walking on sand, correspond to a total speed 5.0 m/h or 48 body lengths per hour.

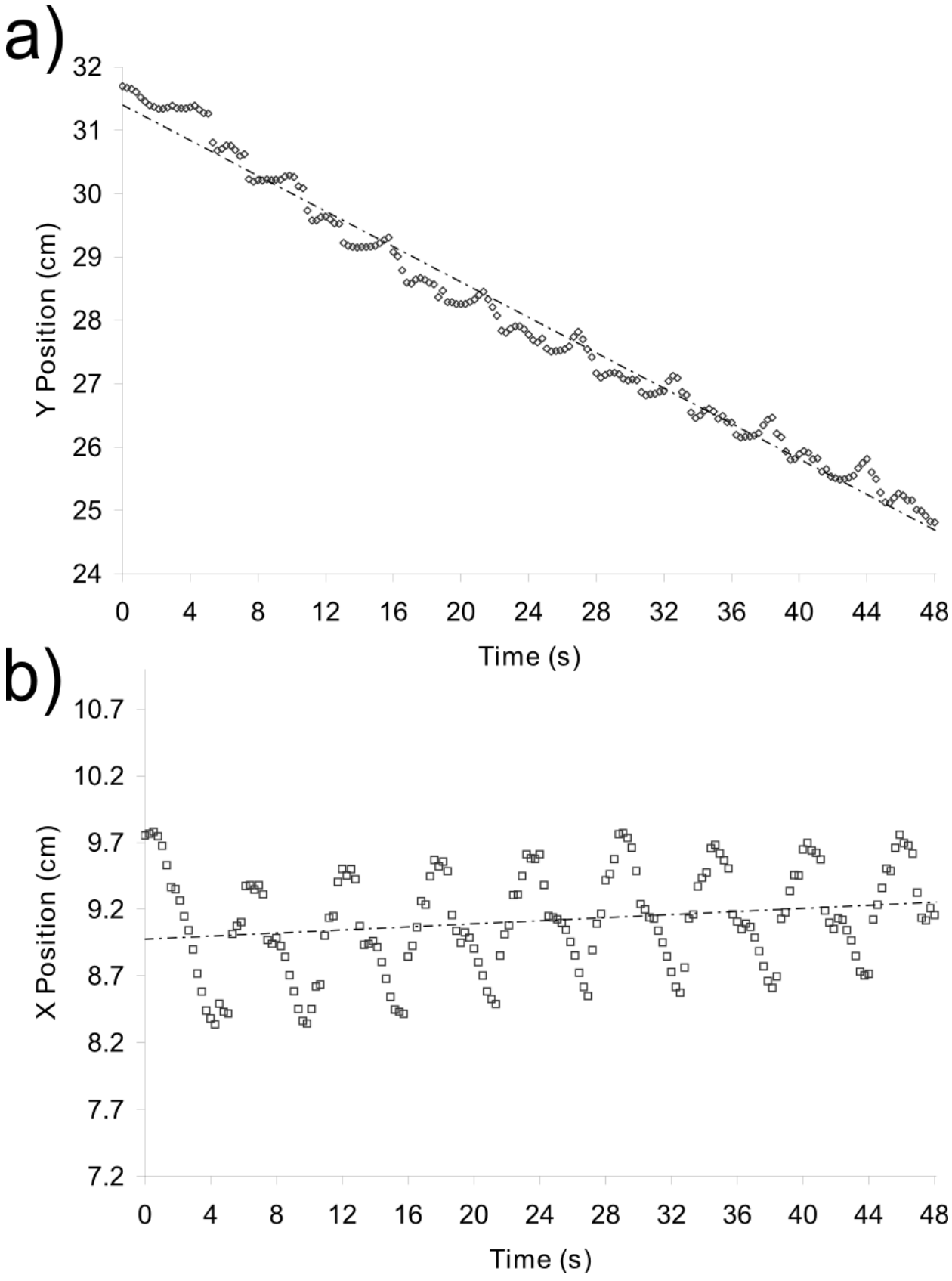
a)
Y Position (cm)
32
31
30
29
28
27
26
25
24
0
4
8
12
16
20
24
28
32
36
40
44
48
Time (s)
b)
X Position (cm)
10.7
10.2
9.7
9.2
8.7
8.2
7.7
7.2
0
4
8
12
16
20
24
28
32
36
40
44
48
Time (s)

Figure S9. A series of still frames from Video S2 shows the legged robot gripping a light bulb. a) The legs are first unactuated and then b) all legs are pressured to grip the light bulb. To show the light bulb remains undamaged, c) the legs are depressurized and the light bulb is released. The tubes corresponding to the tether exit the robotic gripper/walker at the top.

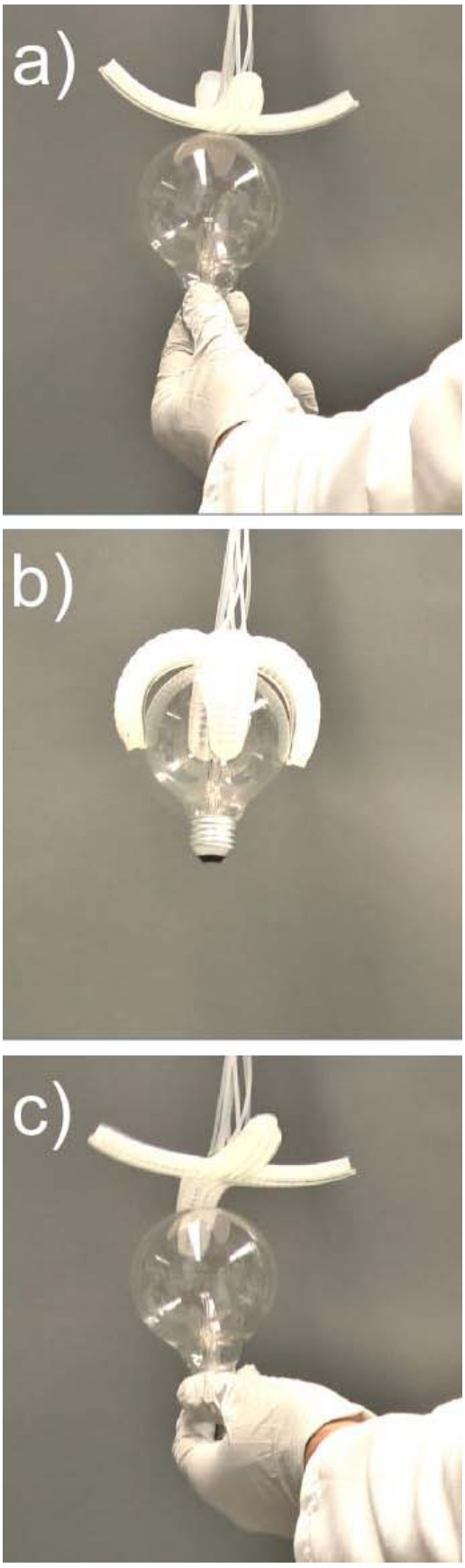
a)
b)
c)

Figure S10. a) Design of the net for the paper-MEMS based bump sensors. Stencil-printed carbon ink patches are used as piezoresistive sensors. Copper wires (not shown) are connected to the sensor using silver epoxy. b) The folded form of the sensor network showing the triangular cross section of the arm and the top-side of the flexible hinge containing the piezo sensor. c) Photograph of the soft robot with the sensor array mounted on the underside. Both the sensor network and the robot measure 15 cm from point to point through their centers.

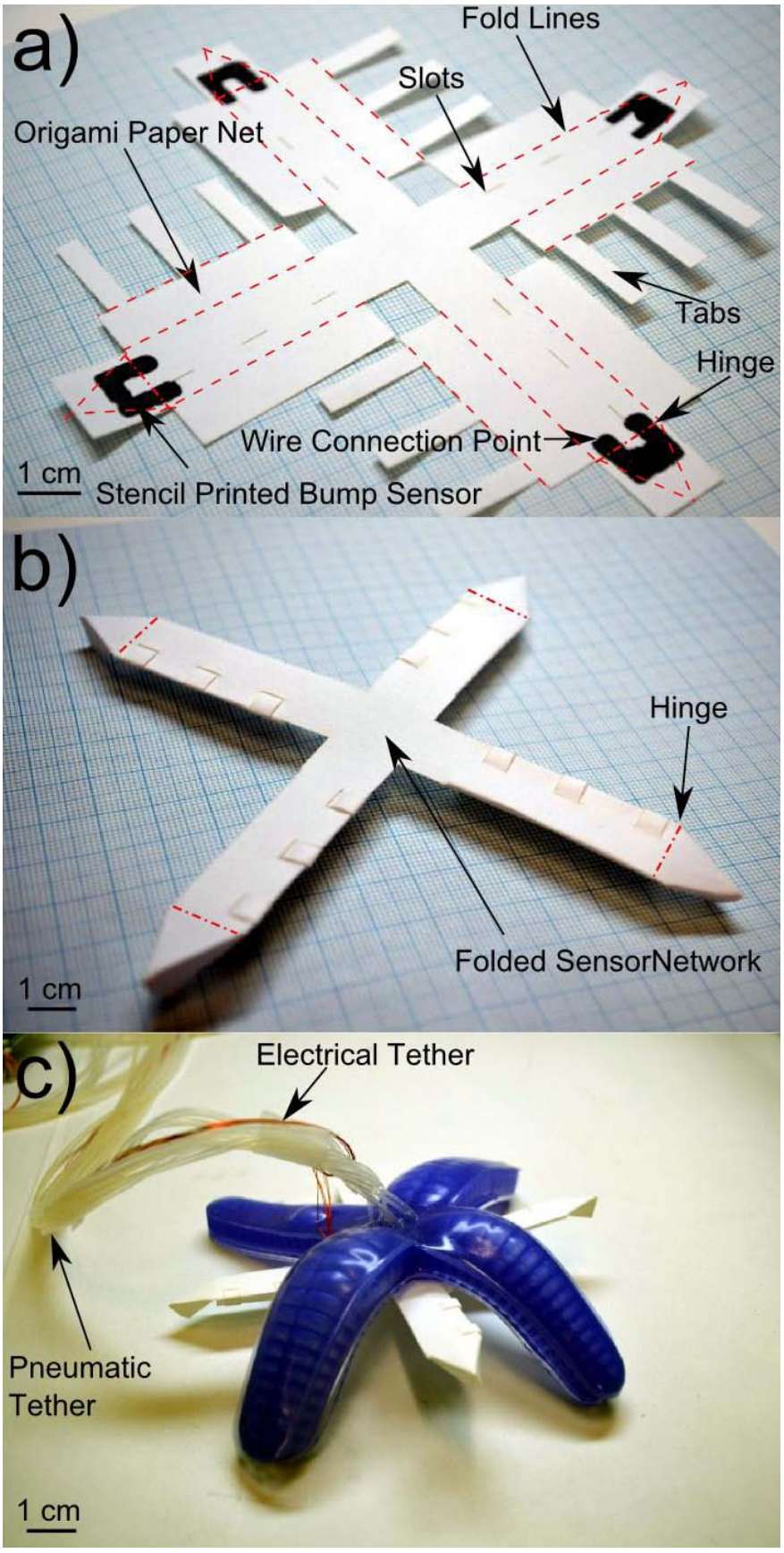
a)
Fold Lines
Slots
Origami Paper Net
Tabs
Hinge
Wire Connection Point
1 cm
Stencil Printed Bump Sensor
b)
Hinge
Folded SensorNetwork
1 cm
c)
Electrical Tether
Pneumatic
Tether
1 cm